Surface tension and elasticity of gel studied with laser-induced surface-deformation spectroscopy

Y. Yoshitake*
Tokyo Denki University, Hatoyama, Hiki-gun, Saitama 350-0394, Japan

S. Mitani and K. Sakai
Institute of Industrial Science, University of Tokyo, 4-6-1 Komaba, Meguro-ku, Tokyo 153-8505, Japan

K. Takagi
Institute of Industrial Science, University of Tokyo, 4-6-1 Komaba, Meguro-ku, Tokyo 153-8505, Japan
(Received 19 September 2007; revised manuscript received 19 July 2008; published 20 October 2008)

The laser manipulation technique was effectively used for agarose solutions and the frequency specstrum of the surface response to the periodical laser irradiation yielded shear elasticity G and surface tension σ in the gel. The laser spot size, from 60 μm to 200 μm in radius, was chosen so that either the Rayleigh waves or the capillary waves, selectively excited, associated with G or σ, respectively. The result of G showed a dependence on the agarose concentration that is consistent with the theoretical prediction of the percolation model, while σ has little dependence on the concentration. The surface state of 0.2 wt. % agarose solution was controlled with sodium-dodecyl-sulfate (SDS) additives, and σ of the gel and the sol was observed at different SDS concentrations: The result showed (i) σ decreased with increasing SDS concentration up to 39×10^{-3} mol/l and kept a constant value thereafter, and (ii) the gel and the sol have the same value of σ and the same dependence on the concentration. These results were considered from a viewpoint of surface pressure and a partially quantitative discussion was made on the surface adsorbed with SDS and agarose molecules.

DOI: 10.1103/PhysRevE.78.041405 PACS number(s): 83.80.Kn

I. INTRODUCTION

The study of surface and interface properties of soft materials provides us with knowledge indispensable in understanding the basic functions of human tissues such as membranes, blood vessels, and other internal organs. In particular, the surface tension on gel is a property of great importance since we have various gelatinous organs at movable parts for reducing the friction. Gel is a liquid with a shape or, in other words, a liquid in microscopic view and a solid in macroscopic view. Smooth motion at knuckles and knees or lubrication of eyelids owes much to the fluidlike aspect of this somewhat amphibious nature inherent in gels. There are many cases in which the surface tension governs the interfacial dynamics in tissue systems.

Current methods for measuring the surface tension are the Whilhelmy plate, sessile drop, and maximum bubble pressure methods, which give a large deformation allowed only for fluids. They are hardly of use for the measuring gels as an elastic matter. On the other hand, there has been proposed a surface wave method that is based on the mechanical excitation and optical detection of the surface tension wave propagating on the medium [1–3]. The dispersion relation of the wave yields the surface tension as well as the viscosity. A more-sophisticated technique of the wave measurement is the ripplon light scattering method, in which ripplon, the thermally excited surface tension wave with the amplitude of nanometer scale, is observed in a dynamic light scattering experiment [4,5]. The spectrum of the scattered light gives the ripplon dispersion, from which the surface tension and viscosity are derived. These wave-propagation methods have been applied also to soft gels with low elasticity [6], though they do not provide us with the effective measurement of surface tension.

We have already established another technique for measuring the surface properties of interest: The laser-induced surface-deformation spectroscopy [7–9]. Though this technique also treats the surface waves in principle, it does not measure the wave propagation, but observes a frequency response of the surface to a mechanical vibration forced by a periodical laser irradiation with a spatial boundary condition. We have successfully applied this method to highly viscous liquids [9], and found that it is useful even when the amplitude damping is so strong that the propagation measurement of ordinary sense is practically inhibited. The major difficulty in gel is that the elastic force suppresses the surface vibration to a very small amplitude. Then this technique would be useful in gels: The surface tension and shear elasticity would be determined from the mechanical impedance of the surface under periodical driving force given by the laser irradiation.

Gel is a solid matter yet far from rigid, and its shape is just kept by the small elasticity for shear deformation. Therefore shear elasticity would be one of the most fundamental properties of gels. The shear elasticity of soft matters has been measured, for example, from the dispersion of shear-mode acoustic waves, from the complex reflectivity of the acoustic waves at the interface of gel and glass, or from the complex mechanical impedance to a given shear deformation [10,11]. The present method has significance also as a technique of elasticity measurement.

This study includes another problem that is interesting from a viewpoint of basic wave phenomena. Generally speaking, gel surface may have two different modes of

*yoshit@mail.dendai.ac.jp

waves, the surface tension (capillary) wave and the surface elastic (Rayleigh) wave [12–14]. Which type of wave actually appears or predominates over the other?

We decided to apply the technique of laser-induced surface-deformation spectroscopy to gels in expectation of measuring the surface tension and the elasticity. As the standard specimen, we chose agarose-water solution of different concentrations with or without the surfactant molecules that change the surface tension.

II. PRINCIPLE AND THEORETICAL BACKGROUND

This technique is comprised of the surface driving by the laser radiation pressure, and the optical probing with another laser that detects the surface motion at the same point. The marked advantage of this method is the noncontact and noninvasive approach to the surface under study: It has no foreign obstacle that is in direct contact with the sample and might possibly cause contaminations or damages. The ripplon light scattering would also have potential to measure the gel surface properties with noncontact and noninvasive approach. However, the amplitude of ripplon attenuates with elasticity increase, and it worsened the measurement accuracy. Compared with this, the laser-induced surface-deformation spectroscopy has good sensitivity because the vibrations are occured by the external energy given by laser light. This method can be used to measure the surface waves on the rigid gel.

When light is incident onto a transparent sample from the air, the optical momentum increases discontinuously since it is proportional to refractive index of the medium. This difference in the momentum gives upward force to the surface as a reaction. Thus, the surface is deformed into a lower-index side and swells up [15]. Displacement and shape of the surface is determined by the balance among the three kinds of force applied to the liquid surface: Radiation pressure, the Laplace force by surface tension of the curved plane, and the gravity force. On the gel surface, the shear elasticity should be added to them as the fourth force. The surface displacement is typically in the order of nanometer [9].

The driving laser is chopped at ω and gives a forced vibration to the surface area with a diameter $2w$, w being the spot radius of the irradiating laser. Then the major wave number of the excited surface wave is $k_w=\pi/2w$ since the area with diameter $2w$ is picked up and makes one-half of the wavelength. Thus we can control both the frequency ω and the wave number k of the surface waves and make a spectroscopic study: The dynamic response of the surface is obtained by varying the chopping frequency. The surface displacement that is as small as nanometer order is sensitively detected with the probe laser illuminating the driving point [7–9].

The surface displacement induced by the laser is given by

$$\xi(r,t) = \frac{w^2 p_0}{4\rho}\int_0^\infty \frac{k^2 e^{-k^2w^2/8} J_0(kr)(e^{i\omega t}-1)}{D(\omega)}dk, \qquad (1)$$

where p_0 is the laser intensity, ρ is the density, and $D(\omega)$ is the dispersion relation of surface wave [9]. For the gelatinous matter with very small elasticity, the dispersion relation has been derived along the line of Harden, Pleiner, and Pincus (HPP) theory [16] that treats the viscoelastic medium as a fluid with complex viscosity. Then

$$D(\omega) = (i\omega + 2\nu k^2)^2 - 4\nu^2 k^4\left(1+\frac{i\omega}{\nu k^2}\right)^{1/2} + \frac{\sigma k^3}{\rho}, \qquad (2)$$

where $\nu=\frac{\eta}{\rho}+\frac{G}{i\omega\rho}$ is the complex kinetic viscosity, σ is the surface tension, and η are the shear elasticity and viscosity, respectively. The surface waves on gels have been treated in the opposite approach as well: Gels are incompressible solid medium with complex elasticity and surface tension [14,17]. The result has given the same dispersion relation as Eq. (2) in the approximation $\eta\sim 0$ [14]. In liquids or sols, kinetic viscosity is simply given by $\nu=\frac{\eta}{\rho}$ with $G=0$, and Eq. (2) is reduced to $D_\sigma=\omega^2-\frac{\sigma k^3}{\rho}$. The equation $D_\sigma(\omega)=0$ yields the well-known form of capillary wave dispersion under the low-viscosity approximation

$$\omega(k) = \sqrt{\frac{\sigma}{\rho}k^3}. \qquad (3)$$

On the other hand, numerical calculation of Eq. (2) with $\sigma=0$ and $\eta=0$ provides a curve that agrees completely with $D_G=\omega^2-(0.9553)^2Gk^2/\rho$, that gives the dispersion relation of the Rayleigh wave,

$$\omega(k) = 0.9553\sqrt{\frac{G}{\rho}}k. \qquad (4)$$

Here, the factor 0.9553 is the value for half-finite elastic medium with Poisson's ratio of 0.5, which is corresponding to the assumption of "incompressible" in these theories.

In the measurement we detect the curvature at the center of the deformed surface. Then, the observed signal is given by the second-order differential of Eq. (1) at $r=0$ and hence $J_0(kr)=1$. Then it is written by

$$\frac{\partial^2}{\partial r^2}\xi(0,t) = \frac{w^2 p_0}{4\rho}\int_0^\infty \frac{k^4 e^{-k^2w^2/8}(e^{i\omega t}-1)}{D(\omega)}dk. \qquad (5)$$

As described later, we use lock-in amplifier to observe the surface response sensitivity. It observes the amplitude of the component with $\exp(i\omega t)$. We carried out the experiment changing ω and obtained the spectrum $S(\omega)$ that is to be correlated with

$$S(\omega) \propto \int_0^\infty \frac{k^4 e^{-k^2w^2/8}}{D(\omega)}dk = \int_0^\infty \frac{k^4 e^{-k^2w^2/8}}{(i\omega+2\nu k^2)^2 - 4\nu^2k^4\left(1+\frac{i\omega}{\nu k^2}\right)^{1/2}+\frac{\sigma k^3}{\rho}}dk. \qquad (6)$$

Equation (6) tells us that the surface motion shows a full response to the driving force at limiting lower frequencies independent of ω. At high frequencies, on the other hand, the surface cannot follow the periodical driving force and gradually freezes. In the intermediate region, the spectrum exhibits

a complicated feature depending on σ, G, and η as shown in the following sections. Roughly speaking, the spectrum shifts to higher frequencies with increasing σ and G, and to lower side with increasing η.

III. EXPERIMENTS

The present system of the laser-induced surface-deformation spectroscopy is almost the same as was used in our previous study [9]. We used a frequency-doubled YAG laser for driving the surface vibration: About 2.0 W output was chopped at ω with an acousto-optic modulator and focused onto the sample surface in the spot of which the radius is $w=60$ μm to 200 μm. The spot size is adjusted by choosing a suitable focal length of the condenser lens. The chopping frequency ranges from 100 Hz to 100 kHz depending on G and σ of the sample. The surface motion at the point was detected with a He-Ne laser. The probe light joints the pump laser on a dichroic mirror located over the sample liquid, and is incident down onto the same spot together with the driving laser. The deformed surface works as a convex mirror and the reflection of the probe beam diverges to a circular pattern. The central intensity of the far-field pattern is observed by a photodiode with a pinhole in its front, and the output signal is detected with a lock-in amplifier to which the chopping signal is given as the phase sensitive reference. The photodiode output is proportional to the surface curvature at the central point except for its sign, and directly gives the spectrum $S(\omega)$ of Eq. (6). About 1 or 2 hours are typically needed to acquire one spectrum. It should be increased by the averaging time so that the high elasticity dilutes the measurement precision.

We studied the aqueous solutions of agarose with different concentrations both in sol and gel states. We prepared the solutions by dissolving the agarose powder purchased from Wako (AGAROSE28CC) into distilled water heated up to ~90 °C. The solutions were cooled down to 40 °C for sol measurement; and gel samples were further cooled and kept at 20 °C ± 1 °C for 6 hours before the experiment.The gelation temperature of this specimen is 26 °C–29 °C at 2 wt. %. For good temperature control, we covered the sample trough with a glass plate which the laser beams pass through. We used a tight lid to seal the atmosphere on the liquid and kept the vapor pressure. The laser light does not cause damage to agarose gel because of it's colorless transparence.

IV. RESULTS AND DISCUSSION

Typical spectra for sol and gel of 0.45 wt. % agarose concentration are shown in Fig. 1, in which (a) and (b) are the result for the same specimen but obtained with different laser spot radius, $w=60$ μm and 100 μm, respectively. The open and the closed circles indicate the spectra for the sol and gel, respectively. They are normalized so that the limiting value at lower frequencies equals unity. The dotted line in both figures shows the curve of Eq. (6) with $G=0$, fitted to the experimental points of the sol. Note that the lock-in signal gives the absolute of Eq. (6). The overall shape of the sol

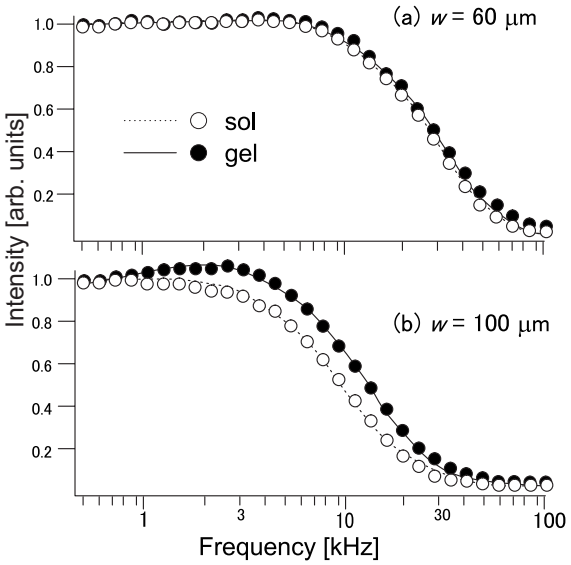

FIG. 1. Frequency spectra in 0.45 wt. % agarose solutions observed with (a) the laser diameter $w=60$ μm and (b) $w=100$ μm. The open and closed circles indicate the results in sol and gel state, respectively. The spectrum for the gel is almost the same as that in the sol in (a), suggesting that capillary waves are excited by the laser irradiation with $w=60$ μm. On the other hand, the gel spectrum in (b) shows a noted difference from that for the sol: The gel surface makes response as an elastic matter to the $w=100$ μm irradiation, and holds Rayleigh waves.

spectrum shows no remarkable difference between (a) and (b) except for its position on the frequency axis. The larger spot size of the driving laser causes a deformation of larger area and shifts the spectrum to the lower frequency side. All the specimens of sol and gel used in this study have viscosity smaller than 10 mPa s, the range where η has little influence on the spectrum. Hereafter, we used a fixed value $\eta=1$ mPa s, the value of water for convenience sake in all of the analysis. Note that 2 times as much value of η gives only 4% frequency shift to the spectrum of both sol and gel when $w=100$ μm.

The spectrum of gel exhibits a substantial difference between (a) and (b). The gel spectrum in (a) is very close to that for the sol. This fact suggests that the gel makes a liquidlike response to the laser irradiation with $w=60$ μm and capillary waves are actually excited despite the elasticity. Furthermore, gel and sol have almost the same surface tension as discussed more precisely in the later section. It should be reminded here that the curves of sol and gel were obtained at different temperatures, 20 °C and 40 °C, respectively. The physical parameters in Eq. (6) generally depend on temperature, yet the two curves almost agree with each other. Of the parameters, σ has a small dependence on T: The decrease in σ of water is less than 4% in the increase of T from 20 °C to 40 °C [18], and the due frequency shift is about 2%, well within the experimental ambiguity. As for the elasticity, G has a finite value in gel, while $G=0$ in sol. The spectra in (a) are in the capillary wave region where G hardly gives influence. Detailed discussion on this problem will be made in the following section. On the other hand, the gel spectrum in (b), obtained with $w=100$ μm, is obviously dif-

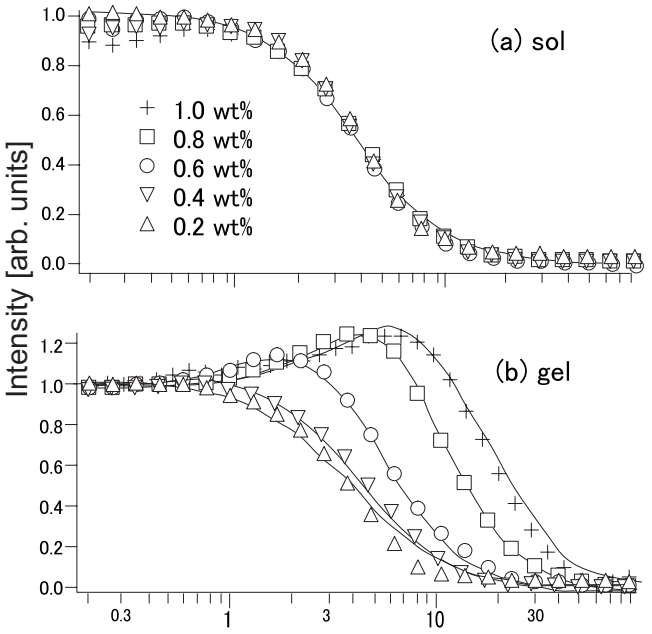

FIG. 2. Frequency spectra observed in the agarose solutions with different concentrations indicated in the figure, in which (a) and (b) show the results for the sol and the gel, respectively, at the same concentration. The solid lines are the fitted curves of Eq. (6). While the sol spectra make no remarkable change, the gel spectra are strongly dependent on the concentration: They shift to higher frequency side with increasing concentrations, and exhibit a broad maximum.

ferent from that for the sol. The elasticity takes a considerable role as the restoring force against the deformation of this scale, and the surface partially behaves as that of elastic matter.

A. Elasticity in gel

One of the purposes of this study is to establish a technique for measuring the elasticity of gels, and the present experiment and the spectrum of Eq. (6) have a potential for yielding G without giving mechanical damage or abuse to the soft and fragile materials. It would be physically natural to assume that gel surface holds Rayleigh waves in the lower wave-number limit where gel behaves as a purely elastic body, while it has capillary waves in the higher limit. This assumption was confirmed by the numerical calculations of Eq. (2) with different values of σ and G. In the very low-wave-number region, the equation $D(\omega)=0$ has a real solution of $\omega(k)$ that approaches to the dispersion relation of Rayleigh waves associated with Eq. (4). In the high-wave-number region, on the other hand, it has a practically real solution that agrees with the dispersion of capillary waves given by Eq. (3). Although the equation $D(\omega)=0$ has a complex solution in the intermediate-wave-number region, its imaginary part decreases and ignores the high-wave-number region [14]. The curves of $\omega(k)$ given by Eqs. (3) and (4) have a crossover point roughly at

$$k^* = G/\sigma. \tag{7}$$

This crossover k^* gives a good measure in presuming the related wave mode: The Rayleigh region at $k \ll k^*$ or the capillary region at $k \gg k^*$. The intermediate region where k is comparable to k^* is involved in complicated wave phenomena discussed later.

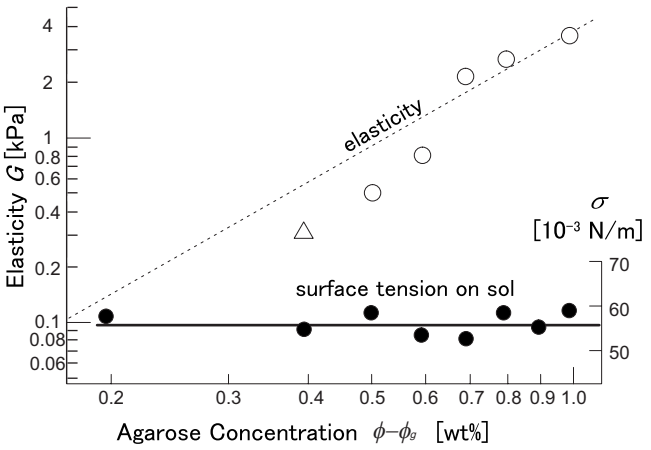

FIG. 3. The elasticity in gel (open circles) and the surface tension on sol (closed circles) at different concentrations determined from the spectra in Fig. 2, and shown on the left-hand and right-hand ordinates, respectively. The triangle point was obtained with $w=200$ μm. The surface tensions are independent of agarose concentrations. The elasticity increases with increasing concentration, and the dashed line represents the theoretical curve $G \propto (\phi-\phi_g)^{\varepsilon}$ with $\phi_g=0.013$ wt. % and $\varepsilon=2.0$, predicted with percolation model [10].

Some of the spectra obtained over the concentration range from 0.2 wt. % to 1.0 wt. % are shown in Fig. 2, where (a) and (b) are the results in sol and gel, respectively. Therefore, the spectra of sols are adjusted by the half-point from the peak intensity to each other, the intensity which varies dramatically provides informations that we want. The gel spectra are normalized to unity not at the half-point but at the lower frequency limit because they compare with each other easily and show broad peaks. The laser spot size was chosen as $w=100$ μm. Though a larger value of w would be preferable in securing the condition for the Rayleigh region, the decreased optical energy density of pump laser decreases the displacement amplitude and hinders the accurate detection. This problem is serious in gels with high elasticity. All the curves of sols in (a) agree with each other in spite of the different concentrations and give almost the same value $\sigma = 56 \times 10^{-3}$ N/m as shown by the closed circles in Fig. 3. We determined the surface tension in the curve fitting of Eq. (6), setting $G=0$ and varying σ as a running parameter. These solutions are in the concentration range that is ready for gelation, and the surface is saturated with the adsorbed molecules of agarose. The increased concentration has little effect on σ giving no appreciable change in the spectrum shape. This fact should be reminded in the later discussion on the surface tension on gel.

The spectra in gels shown in (b) obviously depend on the concentration, and exhibit a typical shape of Rayleigh region in the range thicker than 0.6 wt. %. The broad peak appears reflecting a kind of elastic resonance in a mechanical system. It is natural for the thicker agarose than 0.45 wt. % to be in the Rayleigh region when $w=100$ μm. Elasticity was determined in this region, where the spectrum shape had a strong

dependency on G while it was almost insensitive to σ. Fortunately we knew σ of sol and fixed it as a constant in the curve fitting, assuming gel has the same value as sol. This assumption is supported by the measurement of σ shown in the succeeding section. Then the fitting has only one adjustable parameter G, and gives reliable values. The solid lines in Fig. 2 are the curve of Eq. (6) fitted to the observed spectra. The elasticity thus determined is shown by the open circles in Fig. 3. The triangle at 0.4 wt. % is a result obtained from the measurement with $w=200$ μm. It did not show a meaningful difference with sol and gel when we measured the elasticity of the 0.4 wt. % agarose gel with $w=100$ μm owing to the discussion in Fig. 1. On this account we measured it with larger wavelength. The gel spectra obtained with $w=200$ μm was different from that for the sol. The dotted line in the figure represents the theoretical curve predicted within the framework of critical phenomena in the percolation model: $G \propto (\phi - \phi_g)^{\varepsilon}$ with ϕ_g being the gelation concentration [10]. The critical exponent ε takes a value very close to 2. The line is in good agreement with the experimental points.

B. Surface tension in gel

The experiment for this purpose should be conducted in the capillary region where the broad peak of elastic resonance is absent. The spectrum changes its position sensitively for the small change in σ, while it has a negligible dependence on G. We chose 0.2 wt. % agarose as the specimen, and fixed the laser spot at $w=60$ μm. In order to vary the surface tension of gel, we added sodium dodecyl sulfate (SDS) as a soluble surfactant, whose critical micelle concentration (CMC) is 8.3×10^{-3} mol/l [19]. We prepared SDS-agarose-water solutions whose SDS concentration ϕ_s ranges from $\phi_s=0$ to 6.0×10^{-3} mol/l. An appropriate amount of the surfactant was completely dissolved with a stirrer in the sol state agarose kept at 40 °C. Then we cooled the solution slowly down to 20 °C for gelation, keeping the air on the liquid at the saturation vapor pressure. The gel specimens thus prepared were very homogenous throughout.

The measurements were made both in the sol and gel, of which the spectra for the latter is shown in Fig. 4. We determined the surface tension in the curve fitting of Eq. (6), setting $G=0$ and varying σ as a running parameter. Although the experimental result in Fig. 3 tells that G has a finite value $\sim10^2$ Pa in 0.2 wt. % gel, this difference makes only 10^{-5} increase in the obtained σ. As long as we are in the capillary region, we can safely ignore G and need not know its true value. The obtained surface tension is given in Fig. 5 in which the closed and the open circles indicate the results for the sols and gels, respectively. The triangles indicate σ in sols obtained with the Wilhelmy method. Note that all of the points at the same concentration agree well. It is known that the gelation temperature of polymer gels generally depends on the surfactant concentration and, in agarose solutions, it decreases with increasing surfactant concentration [20,21]. The data points for the gel are absent above 4.0×10^{-3} mol/l, since the gel never appears at 20 °C due perhaps to the interference of thick SDS.

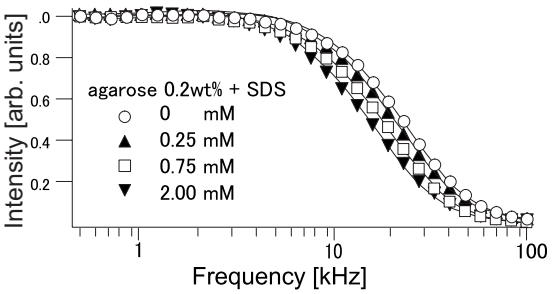

FIG. 4. Frequency spectra of 0.2 wt % agarose gel added with different amounts of SDS. The spectra did not change between gels and sols. Besides 0.2 wt. % gels with (and without) SDS have lower surface tension and lower elasticity than 0.45 wt. % agarose gel, hence it is ensured that they are in the capillary region at $w=60$ μm. The spectra move to the lower frequency side as SDS concentration increases.

An interesting aspect in Fig. 5 is that the open and the closed circles agree well within the experimental error. This result tells us that gelation process does not change the surface tension largely. Is this fact reasonable? The agarose molecules on the surface and in its close vicinity contribute to the decrease of the surface energy by equilibrium adsorption. The adsorption increases the surface pressure and hence decreases the surface tension, which is equivalent with the surface energy. In the gelation process, the free polymers in sol loosely bond themselves with others to make a percolated network structure. Therefore, the change at the surface is not in the number of adsorbed molecules, but in the appearance of a net with large meshes. This difference would give just a higher-order contribution to the surface energy, in comparison with the overwhelming effect of adsorption (net or string). It should be reminded here that the temperature difference between the sol and gel in this study would make a

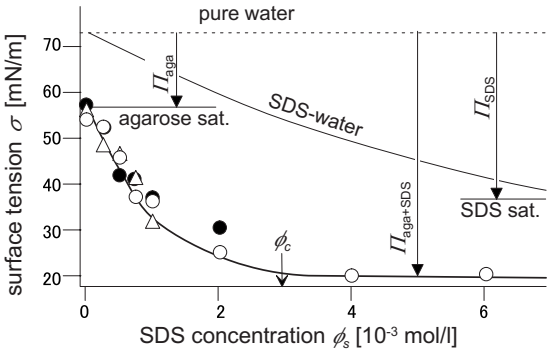

FIG. 5. Effect of SDS addition on the surface tension of 0.2 wt. % agarose solution. The open and the closed circles indicate the measured values for the gel and sol, respectively, and the triangles are those for the sol obtained with the Wilhelmy method. The thick solid line is just a guide for the eye, and ϕ_c is associated with CMC of the agarose solution. The thin solid line shows the curve of surface tension on SDS-water solution. The three horizontal lines indicate, from the top, the surface tension of pure water, that of water surface saturated with the adsorbed agarose, and that of SDS solution above CMC. The three downward arrows show the surface pressure of the different states, from the left, the surface saturated with agarose, with agarose and SDS, and with SDS.

possible difference of 4% in σ, which is within the experimental error as has been already discussed.

The observed surface tension rapidly decreases as ϕ_s increases to $\phi_c=3\times10^{-3}$ mol/l, and takes a constant value thereafter. The thick solid line is just a guide for the eye. This curve reflects the surface state of agarose solution including the surfactant molecules as the second solute. We interpret a static aspect of the adsorption effect, referring to the surface tension of SDS solution in pure water shown by the thin solid curve in Fig. 5. The surface tension of SDS water is $\sigma=72\times10^{-3}$ N/m, the value of pure water, at $\phi_s=0$ mol/l, and decreases monotonously as ϕ_s increases up to CMC (critical micelle concentration) at 39×10^{-3} mol/l, outside the range of Fig. 5 [22]. The water surface is saturated with the adsorbed SDS above CMC and σ has a constant value 39×10^{-3} N/m independently of ϕ_s. The decrease in σ equals the surface pressure Π_{SDS} given by the saturated adsorption of SDS, and $\Pi_{\mathrm{SDS}}=33\times10^{-3}$ N/m is obtained as shown in the figure.

On the curve of SDS agarose water, on the other hand, σ is 56×10^{-3} N/m at $\phi_s=0$ and the difference from σ for the pure water gives the surface pressure, $\Pi_{\mathrm{aga}}=16\times10^{-3}$ N/m, of the saturated adsorption of agarose. We remind the reader that σ of 0.2 wt. % agarose keeps constant in increasing agarose concentration, suggesting the saturated adsorption. There is room left, however, among the large agarose molecules for much smaller SDS to adsorb. As ϕ_s increases, σ decreases since SDS readily occupies the room, which is perfectly filled up and saturated at $\phi_s=\phi_c$: The surface is completely covered both with agarose and SDS above this concentration, and no longer changes the state. The surface pressure of this state should be given by simple summation of Π_{aga} and Π_{SDS}, if we assume that the two kinds of molecules have no direct interaction in between, and the area occupied by one molecule of SDS is not changing between pure water and the solution. In fact $\Pi_{\mathrm{aga}}+\Pi_{\mathrm{SDS}}$ is 49×10^{-3} N/m, and this value agrees very well with the surface pressure $\Pi_{\mathrm{aga+SDS}}=52\times10^{-3}$ N/m given as the deference in σ between pure water and the solution. It is natural to consider that ϕ_c is the CMC of SDS in agarose solutions, or may be apparent CMC. The present result does not necessarily suggest the micelles are formed in agarose solutions, gel in particular. Perhaps the SDS molecules are adsorbed to polymer chains of agarose.

V. CONCLUDING REMARKS

Elasticity and surface tension are the two fundamental properties representing the amphibious nature of gel, a drenched solid and a liquid keeping a shape as well. The ordinary techniques to measure these properties are immediately faced with the difficulty requested by the countering aspect of this paradox. The Wilhelmy method for the surface tension is unsuccessfully disturbed by the elastic force of the solid; and the elasticity measurement from the acoustic shear mode must determine the phase velocity of waves traveling just a skin depth length as in liquids. Nevertheless, this particular substance behaves either as solid or as liquid by a trick of the laser manipulation technique. It chooses the appropriate wave range, Rayleigh region or capillary region.

In the intermediate region of $k\sim G/\sigma$, on the other hand, gel is involved in a complex phenomenon that is troublesome from a viewpoint of measurement [2,13,23], yet presents us with the wave physics of great interest. Although the two modes are equally given energy here, both hardly propagate as coherent waves. While they show the same motion on the surface at least in the small-amplitude approximation, the particle velocity in the subsurface volume is countering each other: Clockwise circular in the former and anticlockwise elliptical in the latter when the wave is going to the right. Thus, the energy given by the laser irradiation is mostly dissipated in this underwater confliction and the surface shows a very reluctant response to the driving force. Though the present technique still retains sensitivity, it would be difficult to separate the effect of G or σ that contribute equally to the wave propagation as the restoring force. Reliable measurements are hardly possible. This is a simple energy loss occurring in the lower-half of the intermediate region with respect to the wave number. In the higher-half that is closer to the capillary region, phase velocity of the capillary mode exceeds that of the elastic shear mode in the bulk, $(k\sigma/\rho)^{1/2}>(G/\rho)^{1/2}$. The momentum conservation is satisfied in the horizontal plane between the surface capillary wave and the bulk shear wave going down obliquely at a certain angle determined by the two wave numbers. Thus a mode conversion takes place and the surface wave leaks the shear wave into the bulk. This problem of leaky surface mode has been theoretically studied [14,24–26] and the shear elastic wave has been experimentally observed.

The leaky wave phenomenon never occurs in a pure elastic medium since Rayleigh mode is always slower than the bulk shear mode. This is unique to the hybrid nature of gel: The subsurface motions forced by the two surface modes, Rayleigh and the capillary, cooperate (not conflict) to generate the coherent shear waves. The apparent mechanical impedance of the surface increases in either case of the confliction or cooperation. We confirmed this fact in the experiment made during the slow cooling and increasing G. In order to check how the wave decays, we detected the signal at a position slightly off the driving point. In fact we found sudden disappearance and reappearance of the signal, associated, respectively, with the shift from the capillary region into the intermediate region, and that from the intermediate to the Rayleigh as G increases. The results and details will be reported in detail elsewhere.

ACKNOWLEDGMENT

This work was supported by Hayashi Memorial Foundation for Female Natural Scientists.

[1] K. Motonaga, K. Hara, H. Okabe, and K. Matsushige, Jpn. J. Appl. Phys., Part 1 **33**, 3514 (1994).
[2] H. Okabe, K. Kuboyama, K. Hara, and S. Kai, Physica B **263**, 73 (1999).
[3] C. Stevot and D. Langevin, Langmuir **4**, 1179 (1988).
[4] J. C. Earnshaw, Appl. Opt. **36**, 7583 (1997).
[5] K. Sakai and K. Takagi, Langmuir **10**, 257 (1994).
[6] H. Kikuchi, K. Sakai, and K. Takagi, Phys. Rev. B **49**, 3061 (1994).
[7] S. Mitani and K. Sakai, Phys. Rev. E **66**, 031604 (2002).
[8] K. Sakai, D. Mizuno, and K. Takagi, Phys. Rev. E **63**, 046302 (2001).
[9] Y. Yoshitake, S. Mitani, K. Sakai, and K. Takagi, J. Appl. Phys. **97**, 024901 (2005).
[10] M. Tokita and K. Hikichi, Phys. Rev. A **35**, 4329 (1987).
[11] M. Watase and K. Nishinari, Rheol. Acta **22**, 580 (1983).
[12] F. Monroy and D. Langevin, Phys. Rev. Lett. **81**, 3167 (1998).
[13] H. Nakanishi and S. Kubota, Phys. Rev. E **58**, 7678 (1998).
[14] Y. Onodera and P. K. Choi, J. Acoust. Soc. Am. **104**, 3358 (1998).
[15] A. Ashkin and J. M. Dziedzic, Phys. Rev. Lett. **30**, 139 (1973).
[16] J. L. Harden, H. Pleiner, and P. A. Pincus, J. Chem. Phys. **94**, 5208 (1991).
[17] J. Jackle and K. Kawasaki, J. Phys.: Condens. Matter **7**, 4351 (1995).
[18] National Astronomical Observatory, Rika Nenpyo (Chorono-logical Scientific Tables), Maruzen Co., Ltd., 1993 (in Japanese).
[19] A. J. Prosser and E. I. Franses, Colloids Surf., A **178**, 1 (2001).
[20] E. E. Braudo *et al.*, Colloid Polym. Sci. **269**, 1148 (1991).
[21] M. H. G. M. Penders, S. Nilsson, L. Piculell, and B. Lindman, J. Phys. Chem. **97**, 11332 (1993).
[22] K. J. Mysels, Langmuir **2**, 423 (1986).
[23] H. Okabe, K. Kuboyama, K. Hara, and S. Kai, Jpn. J. Appl. Phys., Part 1 **37**, 2815 (1998).
[24] P. K. Choi, E. Jyounouti, K. Yamamoto, and K. Takagi, Jpn. J. Appl. Phys., Part 1 **40**, 3526 (2001).
[25] K. Ahn, Y. A. Kosevich, and M. Won Kim, Europhys. Lett. **60**, 241 (2002).
[26] N. E. Glass and A. A. Maradudin, J. Appl. Phys. **54**, 796 (1983).